1-1-2017

Thermodynamics of quasi-2D electron gas at BFO/Si interface probed with THz time-domain spectroscopy

Xiankuan Liu
Shanghai University

Jiadong Zhang
Shanghai University

Zeyu Zhang
Shanghai University

Xian Lin
Shanghai University

Yang Yu
Shanghai University

See next page for additional authors

Thermodynamics of quasi-2D electron gas at BFO/Si interface probed with THz time-domain spectroscopy

Abstract

An interface is constructed based on a bismuth ferrite oxide (BFO) thin film and p-type silicon, and the temperature dependence of the interface properties has been studied systematically using terahertz time-domain spectroscopy. The BFO/Si interface exhibits quasi-two-dimension electron gas (2DEG) transport in the temperature range of 80 to 140 K: the electrons at the interface possess large electron mobility (∼10 6 cm 2 /V s) and long scattering time (∼100 ps). As the temperature is higher than 140 K, an abrupt decrease in THz interface conductivity is observed due to the breakdown of the 2D EG induced by the surface phase transition in the BFO thin film. Our result reveals that the interface formed between BFO and Si provides a special platform for designing and fabricating THz photonic devices.

Disciplines

Engineering | Physical Sciences and Mathematics

Publication Details

Liu, X., Zhang, J., Zhang, Z., Lin, X., Yu, Y., Xing, X., Jin, Z., Cheng, Z. & Ma, G. (2017). Thermodynamics of quasi-2D electron gas at BFO/Si interface probed with THz time-domain spectroscopy. Applied Physics Letters, 111 (15), 152906-1-152906-5.

Authors

Xiankuan Liu, Jiadong Zhang, Zeyu Zhang, Xian Lin, Yang Yu, Xiao Xing, Zuanming Jin, Zhenxiang Cheng, and Guohong Ma

Thermodynamics of quasi-2D electron gas at BFO/Si interface probed with THz time-domain spectroscopy

Xiankuan Liu, Jiadong Zhang, Zeyu Zhang, Xian Lin, Yang Yu, Xiao Xing, Zuanming Jin, Zhenxiang Cheng, and Guohong Ma

Citation: Appl. Phys. Lett. **111**, 152906 (2017);
View online: https://doi.org/10.1063/1.4989667
View Table of Contents: http://aip.scitation.org/toc/apl/111/15
Published by the American Institute of Physics

Thermodynamics of quasi-2D electron gas at BFO/Si interface probed with THz time-domain spectroscopy

Xiankuan Liu,[1] Jiadong Zhang,[1] Zeyu Zhang,[1] Xian Lin,[1] Yang Yu,[1] Xiao Xing,[1] Zuanming Jin,[1,a)] Zhenxiang Cheng,[2] and Guohong Ma[1,a)]
[1]*Department of Physics, Shanghai University, 99 Shangda Road, Shanghai 200444, People's Republic of China*
[2]*Institute for Superconducting and Electronic Materials, University of Wollongong, New South Wales 2500, Australia*

(Received 11 June 2017; accepted 25 September 2017; published online 12 October 2017)

An interface is constructed based on a bismuth ferrite oxide (BFO) thin film and p-type silicon, and the temperature dependence of the interface properties has been studied systematically using terahertz time-domain spectroscopy. The BFO/Si interface exhibits quasi-two-dimension electron gas (2DEG) transport in the temperature range of 80 to 140 K: the electrons at the interface possess large electron mobility ($\sim 10^6$ cm^2/V s) and long scattering time ($\sim$100 ps). As the temperature is higher than 140 K, an abrupt decrease in THz interface conductivity is observed due to the breakdown of the 2DEG induced by the surface phase transition in the BFO thin film. Our result reveals that the interface formed between BFO and Si provides a special platform for designing and fabricating THz photonic devices. *Published by AIP Publishing*. https://doi.org/10.1063/1.4989667

Since the findings of two-dimensional electron gas (2DEG) in $LaAlO_3/SrTiO_3$ (LAO/STO) heterostructures in 2004,[1] interface electronics based on perovskite oxide have attracted much attention in recent years due to the novel electronic, magnetic,[2–8] and superconducting[9,10] phenomena appearing at the interface of double layer perovskite oxide. It is also well known that 2DEG can be formed in semiconductor heterojunctions, for instance, GaAs/AlGaAs has tremendous applications in modern micro-electronics and photonics. The 2DEG formed at the interface of double-layer perovskite oxide is fundamentally different from that formed in the semiconductor heterojunction. If a semiconductor and a perovskite are brought together, a special interface might be formed, and the interface may have some interesting properties that the intrinsic materials do not have. For instance, the interface at LAO/STO shows conducting 2D electron gas,[1] superconducting properties,[9] and the coexistence of superconductivity and ferromagnetism;[5] The interface at graphene/Si[11] and $BiFeO_3$ (BFO)/Si[12] dominates diode-like THz transmission at room temperature. As far as we know, there is little report on the interface properties of a perovskite grown on a semiconductor.[12]

Multiferroic $BiFeO_3$ (BFO) possesses a perovskite structure and exhibits abundance of electronic and magnetic properties with temperature. Specifically, BFO has some attractive features such as large spontaneous polarization in both phases of a single crystal[13,14] and a thin film.[15,16] Phase transitions occurring at 140 and 200 K in the BFO thin film were observed ten years ago.[17–19] The phase transition initially was attributed to the spin reorientation phase transition, i.e., the magnetization of iron ions switches from the *c*-axis to the *a*-axis with the decreasing temperature, which is similar to that in rare-earth orthoferrite.[20,21] Later on, the origin of low temperature phase transition was confirmed as a surface phase transition.[21,22] These suggest that BFO not only has ferromagnetic and ferroelectric properties at room temperature but also may have interesting interface effects between the BFO thin film and other materials at low temperature. In the present study, by depositing the BFO film on a p-type silicon substrate, a heterostructure is constructed based on the BFO/Si interface. The temperature dependent electronic transport properties of the interface are investigated using THz time domain spectroscopy. Our experimental results demonstrated that upon increasing the temperature from 40 to 140 K, the BFO/Si interface shows a sharp increase in carrier mobility, carrier density, and scattering time. Moreover, BFO surface phase transition behavior is also confirmed to occur at around 140 K by monitoring the temperature dependence of THz interface conductivity. Our study reveals that 2D electron gas can be confined at the perovskite/semiconductor interface at proper temperature, which not only can be used to design electronic and photonic devices but also provides a platform to test the fundamental properties of the perovskite itself.

Particularly, La and Nb codoped $BiFeO_3$ (namely $Bi_{0.8}La_{0.2}Fe_{0.99}Nb_{0.01}O_3$, for simplicity, we use "BFO" throughout the text) films were deposited on p-type (001) silicon and (001) MgO substrates by the pulsed laser deposition method, and the BFO/MgO hybrid structure was fabricated as a reference in contrast to its BFO/Si counterpart. It is worth mentioning that the La and Nb codoped BFO film shows a much better electrical polarization than the intrinsic $BiFeO_3$ film by decreasing the leakage current of ferroelectrics.[23] During the deposition of BFO, the substrates of Si and MgO remained at 550 °C and then cooled down to room temperature following rapid thermal processing. During the deposition, the dynamic oxygen flow pressure was kept at 20 mTorr. The details of the sample fabrication have been reported elsewhere.[23] The thickness of the BFO film is about 200 ± 15 nm, and the 0.4 mm-thick silicon substrate was lightly doped by boron to form a p-type semiconductor[24] with a dopant

a)Authors to whom correspondence should be addressed: ghma@staff.shu.edu.cn and physics_jzm@shu.edu.cn

concentration of $\sim 10^{14}\,\mathrm{cm}^{-3}$.[12] The thermodynamic behaviors of the BFO/Si interface were investigated by THz time domain spectroscopy in the transmission configuration. The details of the setup are presented in supplementary material 1.

Figure 1 shows the THz electric field transmission in vacuum (as a reference) and the BFO/Si heterostructure with four selected temperatures. Apart from the main pulse localized around ~15 ps, a weak signal appears around 24 ps, which corresponds to the second reflection (echo pulse) of the main pulse at each temperature. Upon increasing the temperature from 40 to 140 K, the amplitude of the main pulse is seen to decrease, which suggests that the conductivity of the sample increases with temperature. In contrast to the amplitude transmission, the THz phase shows a negative phase shift by increasing the temperature between 40 and 140 K, which suggests that the transmitted amplitude and the phase shift may come from different contributions. Compared to the main pulse, the "echo pulse" exhibits a zero-phase-shift at a low temperature of 40 K, and it undergoes a π phase shift for the cases of 100 K and 140 K, while, at a high temperature of 300 K, the "echo pulse" goes back to the zero-phase-shift again with the main pulse. Supplementary material 3 presents more details about the phase shifts of the "echo pulse" as a function of temperature in the hybrid structure. We have also checked the amplitude transmission and the phase shift of THz signals through a 0.4 mm-Si wafer (p-type) and a BFO thin film on the 0.5 mm-MgO substrate at various temperatures (supplementary material 4). Both the Si wafer and the BFO/MgO heterostructure do not exhibit temperature dependent behavior at the investigated THz frequency. The strong temperature dependence of THz amplitude transmission in the BFO/Si heterostructure suggests that the conductivity change comes from the BFO-Si interface effect, and the conductivity change in individual BFO films and Si substrates with temperature is negligible. In particular, the π phase shift of echo pulses occurring at 100 and 140 K in the hybrid structure indicates that the BFO/Si interface has high conductivity between these two temperatures. Figure 1(b) shows the Fourier transforms of Fig. 1(a) in the time range of 0 to 22 ps; the BFO/Si heterostructure exhibits a broadband frequency modulation with temperature.

Figures 1(c) and 1(d) show the refractive index (n) and absorption (α) of BFO/Si in the temperature range of 40 to 140 K (n and α in the temperature range of 150–300 K are presented in supplementary material 2 and 3. The inset of Fig. 1(c) shows the temperature dependence of n at three selected frequencies of 0.4, 0.7, and 1.0 THz. A non-monotonous temperature dependence of n is observed, and the minimum n occurs in the temperature range between 110 K and 140 K depending on the detecting frequency. The inset of Fig. 1(d) presents the temperature dependence of α at 0.4, 0.7, and 1.0 THz. We observe absorption peaks at around 140 K for all the selected frequencies. The opposite temperature dependent trend between n and α gives a solid evidence that the two parameters arise from different mechanisms in BFO/Si. The interface effect due to the formation of 2DEG dominates the absorption, while carrier transportation between the BFO film and the BFO/Si interface plays an important role in the temperature dependent refractive index. Thus, it is reasonable to ignore the phase term during the calculation of the temperature dependent conductivity of the 2DEG.

In order to understand the thermodynamical formation of the quasi-2DEG at the interface of BFO/Si, we present the schematic diagram of the energy bandgap for isolated BFO and Si, an ideal BFO/p-type Si heterojunction at thermal equilibrium, and the heterojunctions of BFO/Si at 40 K and 100 K, respectively (supplementary material 5). The energy bandgap alignment for the BFO/Si heterostructure is used to illustrate the formation of the 2DEG at the interface. The energy bandgap diagram presented in Fig. S3 (supplementary material, part 3) suggests that the 2DEG can be formed between the BFO and the Si substrate with varying temperatures. THz spectroscopy spectra presented in Fig. 1 can be

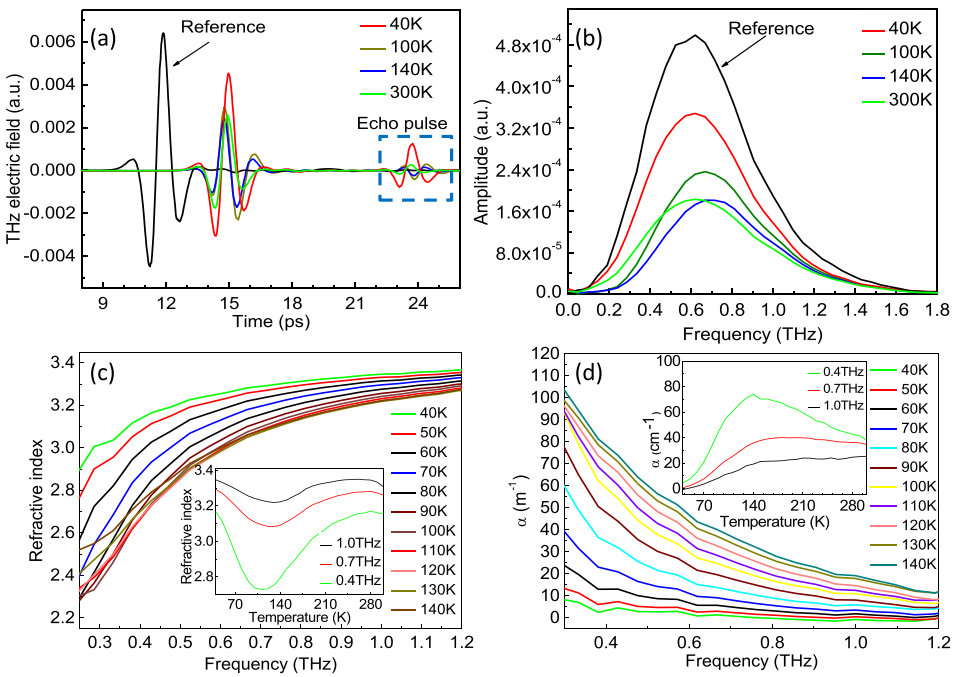

FIG. 1. (a) Transmitted THz electric field of the reference (vacuum) and BFO/Si at selected temperatures of 40, 100, 140, and 300 K. (b) Fourier transform of (a) in the time range of 0 to 22 ps. (c) Refractive index of BFO/Si in the temperature range of 40 to 140 K; the inset shows the refractive index as a function of temperature at three selected frequencies. (d) Absorption coefficient of BFO/Si in the temperature range of 40 to 140 K; the inset shows the absorption coefficient vs temperature at the three selected frequencies.

well interpreted with the temperature dependence of electron transport of the 2DEG. In order to elaborate the 2D electron character further at the BFO/Si interface, electron conductivity, mobility, and scattering time of the 2DEG in BFO/Si are analyzed by THz spectroscopy in the following part. In fact, the anomaly temperature dependence of the refractive index in the BFO/Si hybrid structure is derived from the electron transportation between the BFO film and the BFO/Si interface rather than from the phase shift of the 2DEG. In addition, considering that the 2DEG shows a very large absorption coefficient and very narrow interface space (a few nm), the phase shift of 2DEG can be neglected during the calculation of the conductivity. By taking THz transient at 40 K as a reference, the temperature dependence of conductivity changes of the 2DEG is calculated by[25]

$$\Delta\sigma_{sheet}(\omega) = \frac{2}{Z_0} \times \left[\frac{1}{t(T,\omega)} - 1\right], \tag{1}$$

where Z_0 is the impedance of free space. $t(T,\omega) = \frac{A(T,\omega)}{A(40,\omega)}$ is the THz amplitude ratio between A(T, ω) at temperature T and A(40, ω) at 40 K. Figures 2(a) and 2(b) show the sheet conductivity change of the 2DEG in the temperature range of 50 to 300 K. For clarity, Fig. 2(a) shows the low temperature range of 50 to 140 K and Fig. 2(b) shows the high temperature range of 150 to 300 K (supplementary material 6). It is seen that the dispersion of sheet conductivity changes with temperature shows a different trend in low and high temperature ranges. The solid lines in Figs. 2(a) and 2(b) are the fitting curves with the Drude-Smith model, as given by Eq. (2),

$$\mathrm{Re}\left[\tilde{\sigma}(\omega) = \frac{\varepsilon_0\omega_p^2\tau}{1 - i\omega\tau}\left(1 + \frac{c_0}{1 - i\omega\tau}\right)\right]. \tag{2}$$

Here, ε_0, ω_p, and τ are the permittivity in vacuum, plasma frequency, and carrier scattering time, respectively. c_0 is the backscattering factor (between 0 and -1). $c_0 = 0$ means that all carriers are free, and Eq. (2) is reduced to a Drude model; $c_0 = -1$ means that all carriers are localized. The fitting parameter c_0 as a function of temperature is shown in Fig. 2(c). As the temperature is below 140 K, $c_0 = 0$; c_0 approaches -1 when the temperature is higher than 200 K. From 140 to 200 K, c_0 decreases from 0 to -1 as temperature increases. From the temperature dependence of c_0, we find that the carriers at the BFO/Si interface are free in 2-dimension when the temperature is below 140 K, carriers undergo localization with the increasing temperature, and all carriers are localized when the temperature is higher than 200 K. Figure 2(d) shows the temperature dependence of fitting parameters of plasma frequency ω_p and scattering time τ. Both parameters show a nonlinear temperature dependence. In the low temperature range below 80 K, the magnitudes of ω_p and τ increase with temperature. This process corresponds to the formation process of the 2DEG with temperature. As a matter of fact, the carrier density in the potential well is proportional to $n_0\exp(-e\gamma_b/K_BT)$, with n_0, γ_b, K_B, and T being the carrier density in the BFO thin film, barrier voltage [as shown in Fig. 3(b)], Boltzmann constant, and temperature, respectively. As $T > 80$ K, most of the carriers can overcome the barrier and enter into the potential well and the 2DEG is formed; as a result, the conductivity, plasma frequency, and scattering time show a sharp increase as shown in Fig. 2(d). In the temperature range between 80 and 140 K, both ω and τ increase slightly with temperature, indicating that the 2DEG is stable in this temperature range. Upon increasing the temperature further, both magnitudes of ω and τ show a sharp decrease at around 140 K. When $T > 140$ K, ω and τ decrease slightly with temperature, and the fitting parameters c_0 decrease from zero to negative, which demonstrates that carrier localization occurs at high temperature.

The fitting parameters, ω_p and τ, are also utilized to calculate the carrier mobility ($\Delta\mu$) and *dc* conductivity ($\Delta\sigma_{dc}$) changes of the 2DEG at the BFO/Si interface by $\mu = \frac{e\tau}{m*}$ and $\sigma_{dc}=\varepsilon_0\omega_p^2\tau$, with m* and ε_0 being the effective mass of electrons at the BFO/Si interface and the dielectric constant of vacuum, respectively. As shown in Figs. 3(a) and 3(b), upon

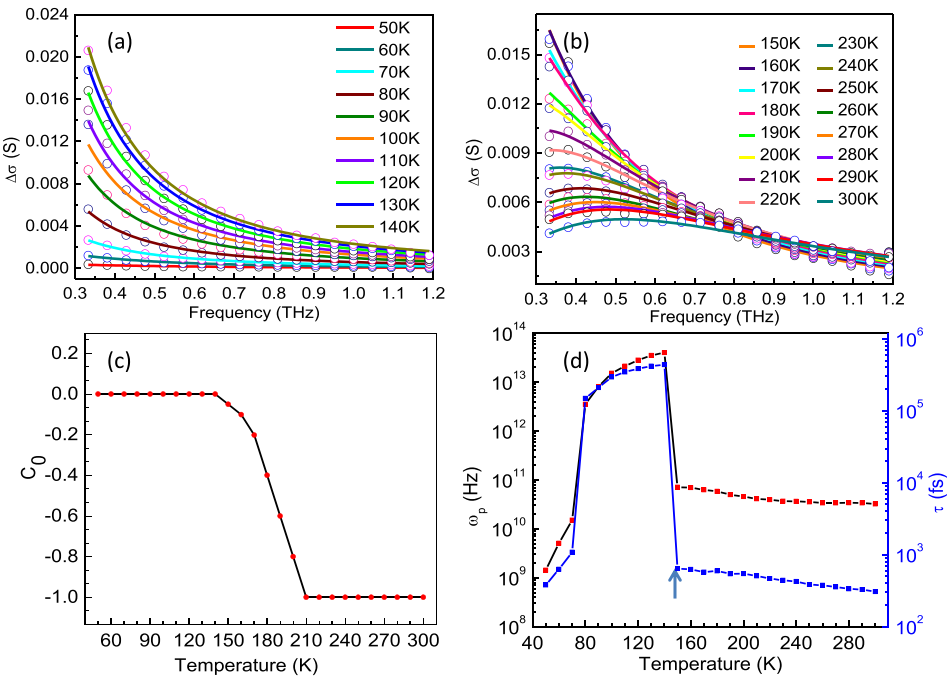

FIG. 2. Interface-sheet conductivity change (color circles) of the BFO/Si (a) from 50 to 140 K and (b) from 150 to 300 K. The solid lines are the fitting curves by Eq. (2). (c) The fitting parameters c_0 are plotted as a function of temperature. (d) The plasma frequency ω_p and scattering time τ are plotted as a function of temperature.

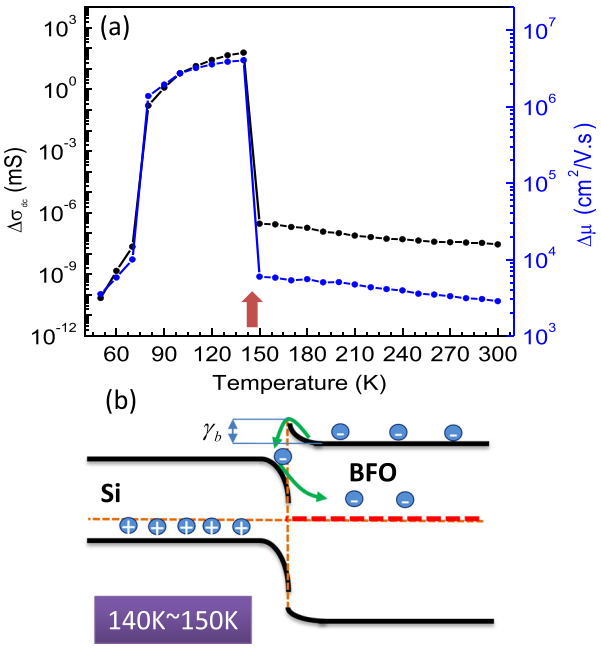

FIG. 3. (a) Electronic *dc* conductivity and mobility changes in BFO/Si from 50 to 300 K. (b) Diagram of the electron tranport process between the BFO film and the BFO/Si interface. The red dashed line in the diagram represents the defect energy level, which crosses over with the Fermi energy at 140 K and above.

the increasing temperature from 50 K to 80 K, a sharp increase in carrier mobility is observed, which reveals the 2DEG formation process at the BFO/Si interface. As $T > 140$ K, more than 3 orders of magnitude of carrier mobility decrease is observed. σ_{dc} shows a similar temperature dependence to μ. Within the temperature range of 80–140 K, the carriers in the heterostructure show large mobility, high *ac* and *dc* conductivity, and long scattering time, and these unique properties of carriers are the strong evidence of the carriers confined in the 2D state.

The carrier transport properties show a sharp decrease as $T > 140$ K, as indicated by arrows in Figs. 2(d) and 3(a), which demonstrate the breakdown of the 2DEG. It is noted that the BFO film undergoes phase transition at ~140 K. It is reasonable to infer that the sharp change in conductivity near 140 K may have close correlation with the phase transition in the BFO thin film. Cazayous *et al.* first reported the phase transition at 140 K, which was assigned to a spin reorientation phase transition in the BFO thin film. Recently, Jarrier *et al.* re-investigated the phase transition of BFO in a wide range of temperatures, and they assigned the transition occurring at 140 K as a surface phase transition.[22] Two main features have been identified for the occurrence of surface phase transition in BFO: (i) a sharp volume change without the actual change in symmetry and (ii) sharp emission of charge (pyroelectric-like current) and maximum in the conductivity of the surface, which are consistent with a crossover between an impurity level and the Fermi level and structural and magnetic disorder at 140 K.[22] As the BFO thin film undergoes the phase transition near 140 K, the Fermi level at the BFO interface may experience an abrupt change and the interfacial defect state below the Fermi level might cross over above it. As shown in Fig. 3(b), the charge is thus released in the defect state of BFO, and the surface charge density in the defect state can be increased greatly above 140 K. As a result, electrons cannot be restricted any more in the potential well formed at the BFO/Si interface. Thus, the THz conductivity shows an abrupt decrease at $T = 140$ K. A first-principles density-functional calculation was performed by determining defects existing on the surface, and the origin of the defects most likely comes from the Bi vacancies.[22]

In summary, by employing THz spectroscopy, we have investigated the temperature dependence of the interface effect of the BFO/Si heterostructure. The heterostructure has a high carrier mobility ($>10^6$ cm^2/V s) and long scattering time (>100 ps) within the temperature range of 80–140 K, suggesting a stable 2DEG phase. The conductivity decreases sharply at $T > 140$ K, which indicates the breakdown of the 2DEG due to the combined effects of 2DEG and surface phase transition in the BFO film. Our results demonstrate that the formation mechanism of 2DEG at the interface of BFO/Si is similar to that in the conventional semiconductor heterojunction. Our findings could provide insights into the understanding of the 2DEG in the double layer perovskite heterostructure and also pave the way toward potential multiferroic/semiconductor hybrid devices with multiple functionalities.

See supplementary material for complete temperature dependent THz spectroscopies of the samples.

This work was supported by the National Natural Science Foundation of China (Nos. 11674213, 11604202, and 61735010), the Young Eastern Scholar (No. QD2015020), the "Chen Guang" project (No. 16CG45), and the Universities Young Teachers Training Funding Program (No. ZZSD15098).

[1]A. Ohtomo and H. Y. Hwang, Nature **427**(6973), 423 (2004).
[2]A. X. Wang, G. Baskaran, Z. Q. Liu, J. Huijben, J. B. Yi, A. Annadi, A. Roy Barman, A. Rusydi, S. Dhar, Y. P. Feng, J. Ding, H. Hilgenkamp, and T. Venkatesan, Nat. Commun. **2**, 188 (2011).
[3]J. A. Bert, B. Kalisky, C. Bell, M. Kim, Y. Hikita, H. Y. Hwang, and K. A. Moler, Nat. Phys. **7**(10), 767 (2011).
[4]L. Li, C. Richter, J. Mannhart, and R. C. Ashoori, Nat. Phys. **7**(10), 762 (2011).
[5]D. A. Dikin, M. Mehta, C. W. Bark, C. M. Folkman, C. B. Eom, and V. Chandrasekhar, Phys. Rev. Lett. **107**(5), 056802 (2011).
[6]M. Gabay and J.-M. Triscone, Nat. Phys. **9**(10), 610 (2013).
[7]L. Weston, X. Y. Cui, S. P. Ringer, and C. Stampfl, Phys. Rev. Lett. **113**(18), 186401 (2014).
[8]D. Doennig and R. Pentcheva, Sci. Rep. **5**, 7909 (2015).
[9]N. Reyren, S. Thiel, A. D. Caviglia, L. Fitting Kourkoutis, G. Hammerl, C. Richter, C. W. Schneider, T. Kopp, A.-S. Rüetschi, and D. Jaccard, Science **317**(5842), 1196 (2007).
[10]Y.-L. Han, S.-C. Shen, J. You, H.-O. Li, Z.-Z. Luo, C.-J. Li, G.-L. Qu, C.-M. Xiong, R.-F. Dou, and L. He, Appl. Phys. Lett. **105**(19), 192603 (2014).
[11]Q. Li, Z. Tian, X. Zhang, R. Singh, L. Du, J. Gu, J. Han, and W. Zhang, Nat. Commun. **6**, 7082 (2015).
[12]X. Liu, Z. Zhang, X. Lin, K. Zhang, Z. Jin, Z. Cheng, and G. Ma, Opt. Express **24**(23), 26618 (2016).
[13]D. Lebeugle, D. Colson, A. Forget, M. Viret, P. Bonville, J.-F. Marucco, and S. Fusil, Phys. Rev. B **76**(2), 024116 (2007).
[14]D. Lebeugle, D. Colson, A. Forget, and M. Viret, Appl. Phys. Lett. **91**(2), 022907 (2007).
[15]J. B. N. J. Wang, J. B. Neaton, H. Zheng, V. Nagarajan, S. B. Ogale, B. Liu, D. Viehland, V. Vaithyanathan, D. G. Schlom, and U. V. Waghmare, Science **299**(5613), 1719 (2003).
[16]W. Eerenstein, F. D. Morrison, J. Dho, M. G. Blamire, J. F. Scott, and N. D. Mathur, Science **307**(5713), 1203 (2005).
[17]M. K. Singh, W. Prellier, M. P. Singh, R. S. Katiyar, and J. F. Scott, Phys. Rev. B **77**(14), 144403 (2008).

[18]M. Cazayous, Y. Gallais, A. Sacuto, R. De Sousa, D. Lebeugle, and D. Colson, Phys. Rev. Lett. **101**(3), 037601 (2008).
[19]M. K. Singh, R. S. Katiyar, and J. F. Scott, J. Phys.: Condens. Matter **20**(25), 252203 (2008).
[20]S. Venugopalan, M. Dutta, A. K. Ramdas, and J. P. Remeika, Phys. Rev. B **31**(3), 1490 (1985).
[21]X. Martí, P. Ferrer, J. Herrero-Albillos, J. Narvaez, V. Holy, N. Barrett, M. Alexe, and G. Catalan, Phys. Rev. Lett. **106**(23), 236101 (2011).
[22]R. Jarrier, X. Marti, J. Herrero-Albillos, P. Ferrer, R. Haumont, P. Gemeiner, G. Geneste, P. Berthet, T. Schülli, and P. Cevc, Phys. Rev. B **85**(18), 184104 (2012).
[23]Z. Cheng, X. Wang, S. Dou, H. Kimura, and K. Ozawa, Phys. Rev. B **77**(9), 092101 (2008).
[24]Z. Jin, Y. Xu, Z. Zhang, X. Lin, G. Ma, Z. Cheng, and X. Wang, Appl. Phys. Lett. **101**(24), 242902 (2012).
[25]J. Lloyd-Hughes and T.-I. Jeon, J. Infrared, Millimeter, Terahertz Waves **33**(9), 871 (2012).